Atmospheric
Chemistry
and Physics
Discussions

Open Access

Simulating the SOA formation of isoprene from partitioning and aerosol phase reactions in the presence of inorganics

R. L. Beardsley and M. Jang

Department of Environmental Engineering Sciences, University of Florida, P.O. Box 116450, Gainesville, FL 32611, USA

Correspondence to: M. Jang (mjang@ufl.edu)

R. L. Beardsley and M. Jang

Title Page	
Abstract	Introduction
Conclusions	References
Tables	Figures
◀◀	▶▶
◀	▶
Back	Close
Full Screen / Esc	
Printer-friendly Version	
Interactive Discussion	

Abstract

The secondary organic aerosol (SOA) produced by the photooxidation of isoprene with and without inorganic seed is simulated using the Unified Partitioning Aerosol Phase Reaction (UNIPAR) model. Recent work has found the SOA formation of isoprene to be sensitive to both aerosol acidity ($[H^+]$) and aerosol liquid water content (LWC) with the presence of either leading to significant aerosol phase organic mass generation and large growth in SOA yields (Y_{SOA}). Classical partitioning models alone are insufficient to predict isoprene SOA formation due to the high volatility of the photooxidation products and the sensitivity of their mass yields to variations in inorganic aerosol composition. UNIPAR utilizes the chemical structures provided by a near-explicit chemical mechanism to estimate the thermodynamic properties of the gas phase products, which are lumped based on their calculated vapor pressure (8 groups) and aerosol phase reactivity (6 groups). UNIPAR then determines the SOA formation of each lumping group from both partitioning and aerosol phase reactions (oligomerization, acid catalyzed reactions, and organosulfate formation) assuming a single homogeneously mixed organic–inorganic phase as a function of inorganic composition and VOC / NO$_x$. The model is validated using isoprene photooxidation experiments performed in the dual, outdoor UF APHOR chambers. UNIPAR is able to predict the experimental SOA formation of isoprene without seed, with H_2SO_4 seed gradually titrated by ammonia, and with the acidic seed generated by SO_2 oxidation. Oligomeric mass is predicted to account for more than 65 % of the total OM formed in all cases and over 85 % in the presence of strongly acidic seed. The model is run to determine the sensitivity of Y_{SOA} to $[H^+]$, LWC, and VOC / NO$_x$, and it is determined that the SOA formation of isoprene is most strongly related to $[H^+]$ but is dynamically related to all three parameters. For VOC / NO$_x$ > 10, with increasing NO$_x$ both experimental and simulated Y_{SOA} increase and are found to be more sensitive to $[H^+]$ and LWC. For atmospherically relevant conditions, Y_{SOA} is found to be more than 150 % higher in partially titrated acidic seeds (NH$_4$HSO$_4$) than in effloresced inorganics or in isoprene only.

R. L. Beardsley and M. Jang

1 Introduction

Volatile organic compounds (VOCs) are emitted into the atmosphere from both biogenic and anthropogenic sources. Once emitted, these compounds react with atmospheric oxidants and radicals to form semi-volatile products that may self-nucleate or partition onto pre-existing particulate matter to form secondary organic aerosol (SOA). Isoprene (2-methyl-1,3-butadiene) is a biogenic VOC with the largest emission of all non-methane hydrocarbons (Guenther et al., 2006), and yet it was initially thought to form insignificant amounts of SOA due to the volatility of its principal oxidation products. This conclusion was supported by early chamber investigations that found isoprene only forms SOA at concentrations much higher than ambient conditions (Pandis et al., 1991; Kamens et al., 1982). However, recent chamber (Edney et al., 2005; Kroll et al., 2005, 2006; Limbeck et al., 2003) and field studies (Claeys et al., 2004; Edney et al., 2005) found that the large emission rate of isoprene makes the contribution to global SOA formation significant even at low yields, and it is estimated that isoprene is the largest single source of global organic aerosol (Henze and Seinfeld, 2006). The proposal of new SOA formation mechanisms, primarily the classical equilibrium partitioning theory by Pankow (1994) and the discovery of aerosol phase oligomerization reactions in the presence of inorganic acids (Jang et al., 2002, 2003), led to the re-examination of the SOA formation potential of isoprene. More recent studies have found the SOA yield of isoprene and its oxidation products to be highly sensitive to aerosol acidity ([H^+]) (Jang et al., 2002; Kuwata et al., 2015; Limbeck et al., 2003; Surratt et al., 2007) and aerosol liquid water content (LWC) (Volkamer et al., 2007, 2009).

The sensitivity of the SOA yield of isoprene to LWC and [H^+] is primarily due to the reactivity of its secondary products. The presence of two double bonds makes isoprene highly reactive and allows for rapid OH initiated oxidation in the atmosphere. The speciation of isoprene photooxidation products and the resultant SOA yields are dependent on NO_x concentrations and atmospheric aging. When NO_x concentrations are low, RO_2 radicals react with HO_2 radicals to form hydroxyperoxides (ROOH) at high

yield. Then, ROOH further react with OH radicals to form dihydroxyepoxides (IEPOX) (Paulot et al., 2009). IEPOX has been found to undergo rapid reactive uptake onto wet ammonium sulfate (AS) inorganic aerosol and acidic inorganic seeds at all RH leading to the formation of tetrols, organosulfates (OS) and other lowly volatile oligomers. In

5 the presence of high NO_x, SOA formation will depend on the ratio of NO_2 to NO with isoprene SOA yields being be higher at large NO_2/NO (Surratt et al., 2010). However, the presence of any significant amounts of NO_x will lead to SOA at lower yields and with less sensitivity to $[H^+]$ and LWC than photooxidation under low NO_x conditions.

In order to quantify and understand the impact of SOA on climate and human health,

10 the prediction of SOA formation of isoprene is essential. SOA models have been developed and utilized to predict the SOA formation of various VOC systems. The two-product model was developed based on classical partitioning theory (Pankow, 1994) and represents SOA formation through use of two or more representative secondary products of varying vapor pressure (Odum et al., 1996). By fitting the stoichiometric and

15 partitioning coefficients of each representative semi-volatile organic compound (SVOC) to experimental data, the SOA yield of a VOC is predicted as a function of the absorbing organic mass (OM) concentration without considering the numerous gas phase products. The simple and efficient handling of SOA mass formation from partitioning by the two-product model led to its widespread use in regional and global models.

20 Nevertheless, the two-product model and its predecessors are limited in their ability to predict SOA formation from aerosol phase reactions in the presence of inorganic aerosol due to the loss of individual product structures, which determine reactivity in the aerosol phase, and the need to fit new parameters for variations in atmospheric conditions. Many models have already incorporated different sets of parameters for

25 each VOC under high and low NO_x regimes, but cannot handle the variations seen in ambient aerosol LWC and $[H^+]$ that enhance SOA formation via aerosol phase reactions (Carlton et al., 2009). In this study, the Unified Partitioning-Aerosol Phase Reaction (UNIPAR) model, which was previously developed and applied to aromatic VOCs (Im et al., 2014), was updated and expanded to model the SOA formation of isoprene

in the presence of high VOC/NO$_x$ (due to the high sensitivity to [H$^+$] in the low NO$_x$ regime) and aerosol acidity under ambient temperature (T) and relative humidity (RH). The model was validated using experimental data from outdoor chamber runs and the results and conclusions are discussed.

2 Experimental methods

Isoprene SOA photooxidation experiments were performed in the University of Florida Atmospheric PHotochemical Outdoor Reactor (UF-APHOR) chambers over the period of a day. The dual 52 m^3 Teflon film chambers were operated simultaneously to allow for investigation of two different experimental conditions under the same ambient, diurnal profiles of sunlight, RH, and T. The chamber air was cleaned using air purifiers (GC Series, IQAir) for 48 h prior to each experiment. In the experiments in which inorganic seeds were used, a 0.01 M aqueous solution of H$_2$SO$_4$ (SA) was atomized using a nebulizer (LC STAR, Pari Respiratory Equipment) with clean air flow. Next, the desired volume of NO (2 % in N$_2$, Airgas) was injected into the chamber and finally, isoprene (99 %, Sigma Aldrich) and CCl$_4$ (> 99.9 %, Sigma Aldrich) were injected using a glass manifold with clean air. CCl$_4$ was used as a tracer for dilution. All chemical species were injected early enough to allow for stabilization and measurement before reactions begun with sunrise. The experimental conditions for each of the chamber runs is shown in Table 1.

To allow for gas and aerosol phase characterization, chamber air is pumped through a number of sampling lines into the lab that is located directly below the roof. Gas phase concentrations of NO$_x$, O$_3$, and SO$_2$ were measured using a Teledyne Model 200E Chemiluminescence NO-NO$_x$ Analyzer, Model 400E Photometric O$_3$ Analyzer, and Model 102E Fluorescence TRS Analyzer, respectively. A HP 5890 Gas Chromatography-Flame Ionization Detector was employed with an oven temperature of 40 °C to measure isoprene and CCl$_4$ concentrations. A semi-continuous OC/EC carbon aerosol analyzer (Sunset Laboratory, Model 4) following the NIOSH 5040 method

was utilized to measure organic carbon (OC) mass concentration ($\mu g\,C\,m^{-3}$), and then converted to OM using an OM/OC ratio of 2.2 (Aiken et al., 2008; Kleindienst et al., 2007). Particle number and volume concentrations were measured with a scanning mobility particle sizer coupled with a condensation nuclei counter (TSI, Model 3025A and Model 3022). Particle wall loss was corrected using size-dependent first order rate constants determined by a chamber characterization with inorganic seed. A Particle into Liquid Sampler (Applikon, ADI 2081) coupled to Ion Chromatography (Metrohm, 761Compact IC) (PILS-IC) was used to quantify aerosol phase inorganic ions. The C-RUV technique (Jang et al., 2008; Li et al., 2015; Li and Jang, 2012) was used to measure [H^+] throughout the experiment. A more detailed explanation of the experimental design and chamber operation can be found in Im et al. (2014).

3   Model description

UNIPAR simulates the SOA formation of VOC photooxidation products from both partitioning and aerosol phase reactions as a function of VOC / NO_x. The photooxidation of the VOC is predicted explicitly offline, and products are lumped using their volatility and reactivity in aerosol phase reactions (Sect. 3.1). SOA formation is then predicted for the lumped species dynamically as a function of the inorganic aerosol composition ([H^+], LWC). The inputs of the model are the consumption of isoprene (ΔISO), VOC/NO_x, the change in aerosol phase sulfate ($\Delta[SO_4^{2-}]$) and ammonium ions (ΔNH_4^+), T and RH at each time step ($\Delta t = 3$ min).

The overall model schematic is shown in Fig. 1. In order to account for effects of inorganic aerosol, isoprene SOA formation is approached in two ways: SOA formation in the presence of deliquesced inorganic seed ($SO_4^{2-} > 0$ and RH > ERH), and either isoprene only ($SO_4^{2-} = 0$) or effloresced inorganic seed ($SO_4^{2-} > 0$ and RH < ERH) (Sects. 3.2 and 3.3). First, the total products originating from ΔVOC in each Δt are split among the lumping groups (i) and combined with the remaining gas phase concentra-

tions from previous steps to get the total gas phase concentration ($C_{g,i}$) (Sect. 3.1). Then the concentrations in the aerosol phase ($C_{mix,i}$) are calculated based on aerosol phase state. Using the estimated $C_{mix,i}$ and inorganic aerosol composition, the OM formation from aerosol phase reactions (OM_{AR}) is calculated (Sect. 3.3.1). OM_{AR} includes SOA formation from oligomerization, acid-catalyzed reactions, and OS formation (Sect. 3.3.2). OM_{AR} is assumed to be non-volatile and irreversible. Finally, the OM from partitioning (OM_P) is predicted using the module developed by Schell et al. (2001) modified to account for the assumed non-volatility and irreversibility of OM_{AR} (Sect. 3.3.3).

3.1 Gas phase photooxidation and lumping structure

The photooxidation of isoprene was simulated using the Master Chemical Mechanism v3.2 (Saunders et al., 1997, 2003) within the Morpho kinetic solver (Jeffries et al., 1998). Simulations were performed under varying VOC/NO_x ratios (ppbC ppb^{-1}) using the sunlight, temperature, and RH data from 23 April 2014. All of the simulations began with NO and begin with sunrise. The sunlight, RH, and temperature profiles used can be seen in the Supplement as well as an example gas phase simulation with corresponding experimental data (Sect. S1).

The predicted photooxidation products are then lumped in UNIPAR using vapor pressure (m, 8 bins) and reactivity (n, 6 bins). The lumping structure is shown in Fig. S3 in the Supplement including the structure of the product which contributes most to each lumping group. The subcooled liquid vapor pressure of each product ($p_{L,i}^{o}$) is estimated using a group contribution method (Joback and Reid, 1987; Stein and Brown, 1994; Zhao et al., 1999), which is explained in detail in Im et al. (2014). The reactivity of each product is estimated based on the number of reactive functional groups. The reactivity bins used in UNIPAR are very fast (VF, α-hydroxybicarbonyls and tricarbonyls), fast (F, 2 epoxides or aldehydes,), medium (M, 1 epoxide or aldehyde), slow (S, ketones), partitioning only (P), and organosulfate precursors (OS_P, 3 or more alcohols). In order to account for the reactivity, glyoxal was allocated to group 6F instead of 8F and

methylglyoxal was moved from 8 to 6 M based on their apparent Henry's constant (Ip et al., 2009). In addition to these reactivity bins, isoprene required the designation of a medium reactivity, multi-alcohol (M-OS$_P$) bin due to the large number of secondary products which contain both three or more alcohols and reactive functional groups (epoxide or aldehyde). Tetrol precursors (IEPOX), which are produced at high concentrations in the gas phase under high VOC/NO$_x$ (low NO$_x$), were also given a separate reactivity bin in order to more easily quantify the SOA formation of these products predicted by the model. The concentrations of each lumping group were set at the peak HO$_2$/NO ratio, which generally corresponds with the majority of SOA formation and represents a shift from less oxidized to more oxidized products. The corresponding stoichiometric mass coefficients ($\alpha_{m, n}$) of each i were then fit to the initial VOC/NO$_x$ ratio. At higher NO, it takes longer to reach the peak HO$_2$/NO ratio and SOA formation is also slower. Figure 2 shows the filled lumping structure at VOC/NO$_x$ of 25 illustrating the high volatility and reactivity of the majority of isoprene products.

3.2 Aerosol composition and phase state

Tropospheric aerosols have been shown to be primarily composed organic compounds and inorganic sulfate partially or wholly titrated with ammonia (Bertram et al., 2011; Murphy et al., 2006). Under ambient diurnal patterns of RH, these aerosols may effloresce and deliquesce, and can be liquid–liquid phase separated (LLPS) or a single homogeneously mixed phase (SHMP) influencing the amount and composition of SOA formed. While dry, effloresced inorganic salts simply act as a seed for organic coating by SOA, deliquesced seeds contain liquid water into which reactive, soluble compounds can dissolve and further react producing lowly volatile SOA (Hennigan et al., 2008; Lim et al., 2010; Volkamer et al., 2007). Furthermore, the SOA composition will determine the phase state of wet aerosol. In LLPS aerosol, hydrophobic SVOC will partition primarily into the organic liquid phase, while a significant fraction of hydrophilic SVOC may dissolve into the salted liquid phase. The RH at which these

transitions occur depends on the concentration and composition of the inorganic and organic components of the aerosol.

Bertram et al. (2011) semi-empirically predicted the efflorescence RH (ERH), deliquescence RH (DRH), and the RH of LLPS (SRH) by fitting experimental data of a number of oxygenated organic-AS systems to the oxygen to carbon atomic ratio (O : C) and to the organic to sulfur mass ratio (org:sulf) of the bulk aerosol. UNIPAR utilizes these parameterizations to predict ERH and DRH at each time step ($t = j$) using modeled O : C and org:sulf from the previous time step ($t = j - 1$). In regards to phase state, UNIPAR is run assuming a SHMP for all of the isoprene simulations due to literature O : C values of isoprene ranging from 0.69 to 0.88 (Bertram et al., 2011; Chen et al., 2011; Kuwata et al., 2013), which corresponds to a SRH of zero.

The interaction of organics and inorganics in SHMP SOA may alter the dissociation of inorganic acids and the resulting [H$^+$]. In order to estimate the impact of organics on [H$^+$] in SHMP isoprene SOA, the percent dissociation of H_2SO_4 was determined using AIOMFAC in the presence of varying amounts of tetrol and hexane, which represent polar and non-polar organic species, under controlled RH. The change in percent dissociation was less than 15 % when compared to inorganic only aerosol at the same RH (details in th Supplement, Sect. S2). Based on these results, it was assumed that presence of organics in isoprene SHMP SOA does not significantly influence the [H$^+$] from inorganic acids. Therefore, [H$^+$] is estimated for each time step by E-AIM II (Clegg et al., 1998) corrected for the ammonia rich condition (Li and Jang, 2012) as a function of [SO_4^{2-}], [NH_4^+], and RH. Then, [H$^+$] is diluted using the ratio of the inorganic volume to the total aerosol volume. The inorganic associated LWC is also calculated using E-AIM II. The LWC of isoprene SOA is estimated in AIOMFAC using the hygroscopic growth factor of a representative isoprene SOA: 20 % sucrose by mass (Hodas et al., 2015) as a surrogate for tetrol and 80 % isoprene derived oligomers (Nguyen et al., 2011). The estimated growth factor is approximately 30 % of that of AS and so, in the model the LWC of isoprene is estimated to be 0.3 of the LWC of AS without an ERH.

3.3 SOA formation

In simulating the total OM (OM_T) from isoprene photooxidation, UNIPAR predicts the SOA formation for each i from both partitioning ($OM_{P,i}$) and aerosol phase reactions ($OM_{AR,i}$). In the previous applications of UNIPAR for aromatic VOC (Im et al., 2014), SOA formation was modeled under the assumption of LLPS aerosol because aromatic SOA is relatively non-polar, and thus aerosol phase concentrations of i were calculated by means of a mass balance between the concentrations in the gas phase, the inorganic aerosol phase, and the organic aerosol phase. In modeling isoprene SOA formation in the presence of a SHMP aerosol, the total concentration ($\mu g\,m^{-3}$ of air) of each lumping species ($C_{T,i}$) was split solely between $C_{g,i}$ and $C_{mix,i}$ by a single gas-particle partitioning coefficient, $K_{mix,i}$ ($m^3\,\mu g^{-1}$),

$$C_{T,i} = C_{g,i} + C_{mix,i}, \tag{1}$$

$$K_{mix,i} = \frac{C_{mix,i}}{C_{g,i}M_{mix}}, \tag{2}$$

where M_{mix} is the total suspended matter and is the sum of the inorganic mass (M_{in}) and OM_T. $C_{mix,i}$ and $C_{g,i}$ can be determined by combining Eqs. (1) and (2) as follows,

$$C_{mix,i} = C_{T,i}\left(\frac{K_{mix,i}M_{mix}}{1 + K_{mix,i}M_{mix}}\right) \tag{3}$$

$$C_{g,i} = C_{T,i}\left(\frac{1}{1 + K_{mix,i}M_{mix}}\right) \tag{4}$$

Calculation of $K_{mix,i}$ follows the gas-particle absorption model (Pankow, 1994).

$$K_{mix,i} = \frac{7.501\,RT}{10^9 MW_{mix}\gamma_{mix,i}p_{L,i}^o}, \tag{5}$$

where R is the gas constant ($8.314\,\mathrm{J\,K^{-1}\,mol^{-1}}$), T is the temperature (K), $\mathrm{MW_{mix}}$ is the average molecular weight ($\mathrm{g\,mol^{-1}}$) of the SHMP aerosol, $\gamma_{\mathrm{mix},i}$ is the activity coefficient of the lumping species in the SHMP aerosol, and $p^{o}_{\mathrm{L},i}$ is the sub-cooled liquid vapor pressure (mmHg) of i. $\gamma_{\mathrm{mix},i}$ accounts for the non-ideality in the SHMP aerosol and allows for more accurate representation of the differences in solubility in the aerosol phase. $\gamma_{\mathrm{mix},i}$ will vary between partitioning species due to differences in polarity and molar volume ($V_{\mathrm{mol},i}$), and also over time due to changes in LWC and aerosol composition.

In order to handle the range of possible $\gamma_{\mathrm{mix},i}$ in SHMP isoprene SOA, the AIOM-FAC model was run using the highest concentration product of each lumping group in the presence of a mixed isoprene SOA/AS aerosol. The representative isoprene SOA composition was chosen based on the results of Nguyen et al. (2011). The bulk organic to sulfur mass ratio (org : sulf), concentration of i, and the RH were varied to cover the range of experimental values, and the resulting $\gamma_{\mathrm{mix},i}$ were fit to the bulk aerosol org : sulf, ln(RH), and lumping species $V_{\mathrm{mol},i}$ and O : C$_i$ using a polynomial equation. The resulting parameterizations are shown in the Supplement along with the predicted $\gamma_{\mathrm{mix},i}$ plotted against $\gamma_{\mathrm{mix},i}$ from AIOMFAC (Sect. S3). In the absence of inorganic aerosol ($[\mathrm{SO_4^{2-}}] = 0$) or in the presence of dry inorganic aerosol, partitioning is assumed to be ideal with organic only partitioning coefficient ($K_{\mathrm{or},i}$) calculated using $\gamma_{\mathrm{mix},i}$ of 1 (Jang and Kamens, 1998) (Fig. 1).

3.3.1 OM from aerosol phase reactions (OM$_{AR}$)

Once $C_{\mathrm{mix},i}$ is determined for each Δt, the OM$_{\mathrm{AR}}$ formation of i is estimated in UNIPAR assuming a second-order dimerization reaction as is shown in Eq. (5),

$$\frac{\mathrm{d}C'_{\mathrm{mix},i}}{\mathrm{d}t} = -k_{\mathrm{AR},i}C'^{2}_{\mathrm{mix},i}. \tag{6}$$

where $C'_{\text{mix},i}$ is the aerosol phase concentration of i in mol L^{-1} of medium and $k_{\text{AR},i}$ is the aerosol phase reaction rate of i (L mol^{-1} s^{-1}). $k_{\text{AR},i}$ (Eq. 6) is calculated each time step using the semi-empirical model developed by Jang et al. (2005) as a function of the reactivity, II (VF, F, M, S; Sect. 3.1), and pK$_{\text{BH+}}$ of i in the aerosol phase, [H$^+$] and

5 LWC (activity of water, a_w) from the inorganic thermodynamic model (Sect. 3.2), and the excess acidity, X (Im et al., 2014; Jang et al., 2006).

$$k_{\text{AR},i} = 10^{(0.0005 \cdot \text{pK}_{\text{BH+}} + y \cdot X + 1.3 \cdot \text{II} + \log(a_w[\text{H}^+]) - 5.5)} \tag{7}$$

All of the coefficients of Eq. (6) were fit using the flow reactor experimental sets for aerosol growth of model organic compounds (various aldehydes) on acidic aerosol

10 (SO$_4^{2-}$–NH$_4^+$–H$_2$O) within the LLPS module and tested for LLPS aerosol (toluene SOA and 1,3,5-trimethylbenzene SOA) by Im et al. (2014), except for the factor y for X. In the presence of deliquesced inorganics, $k_{\text{AR},i}$ is a function of X, which represents the effect of an acidic inorganic medium on the reaction of the protonated organics that act as an intermediate for acid-catalysed reactions. For LLPS aerosol, the protonated

15 organic compounds are in highly concentrated inorganic liquid with high X. The mixture of organic and inorganic species in SHMP aerosol will lead to a modification of X and thus the reaction rate of protonated organics. To account for this change in isoprene SOA, y was determined to be 0.49 by fitting the OM$_T$ of experimental set SA1 (Table 1). In the absence of deliquesced inorganic species, [H$^+$] and X approach zero making

20 $k_{\text{AR},i}$ primarily a function of the reactivity (II) of i.

Then by assuming that OM$_{\text{AR}}$ is non-volatile and irreversible, ΔOM$_{\text{AR},i}$ can be calculated as the reduction in $C_{\text{T},i}$ for each time step (Eq. 6),

$$\Delta \text{OM}_{\text{AR}} = -\sum_i \Delta C_{\text{T},i} = -\sum_i \int \frac{\text{d}C_{\text{T},i}}{\text{d}t}. \tag{8}$$

Combining Eqs. (1)–(6) and solving the second-order ODE provides the analytical solution utilized in UNIPAR (Eq. 7),

$$\Delta OM_{AR} = -\sum_i \frac{k_{AR,i}\beta_{3,i}C_{T,i}^2\Delta t}{1 + k_{AR,i}\beta_{3,i}C_{T,i}\Delta t}, \tag{9}$$

where $\beta_{3,i}$ is equal to

$$\beta_{3,i} = \frac{K_{mix,i}^2 M_{mix}\rho_{mix}10^3}{MW_i(1 + K_{mix,i}M_{mix})^2}. \tag{10}$$

3.3.2 OS formation

Sulfuric acid produced from the photooxidation of SO_2 influences aerosol phase state and hygroscopicity (Sect. 3.2), and acts as a catalyst in OM_{AR} formation. It can be wholly or partially titrated by ammonia, or it can react with reactive organic compounds to form OS. The formation of OS from the esterification of $[SO_4^{2-}]$ with reactive organic functional groups leads to a reduction in $[H^+]$ and LWC influencing subsequent OM_{AR} formation (Im et al., 2014). Therefore, the formation of OS must be estimated in order to accurately predict SOA growth. Of the total $[SO_4^{2-}]$ present in the SHMP aerosol, we assume that the sulfate which is not associated with ammonium ($[SO_4^{2-}]_{free} = [SO_4^{2-}] - 0.5[NH_4^+]$) can form OS. The fraction of $[SO_4^{2-}]_{free}$ that forms OS is calculated using Eq. (10),

$$\frac{[SO_4^{2-}]_{OS}}{[SO_4^{2-}]_{free}} = 1 - \frac{1}{1 + f_{OS}\frac{N_{OS}}{[SO_4^{2-}]_{free}}}. \tag{11}$$

where f_{OS} is a semi empirical parameter determined to be 0.07 by Im et al. (2014) by fitting the $[H^+]$ predicted by UNIPAR to the measured $[H^+]$ in toluene SOA, as a measure of OS formation, using the method of Li et al. (2015). The experimentally determined f_{OS} was validated for isoprene SOA using the experimental data of this study

(Sect. 4.1). N_{OS} is the number of OS forming functional groups present in the aerosol phase. The functional groups that have been shown to form OS are alcohols (Minerath et al., 2008; Zhang et al., 2012), aldehydes (Liggio et al., 2005), and epoxides (Surratt et al., 2010). Alcohols and aldehydes can react with $[SO_4^{2-}]$ in a single position, while epoxides open in the aerosol phase and react with $[SO_4^{2-}]$ in two positions. The average number of $[SO_4^{2-}]$ reaction positions is determined for each i, and then N_{OS} is calculated as the product of the molar concentration of i and the reaction positions of i. Finally, $[SO_4^{2-}]_{OS}$ is removed from $[SO_4^{2-}]_{free}$ so that LWC and $[H^+]$ can be recalculated for the next time step. As OS forms, both LWC and $[H^+]$ are reduced.

3.3.3 OM from partitioning (OM$_P$)

After OM_{AR} formation, $OM_{P,i}$ is calculated using the module developed by Schell et al. (2001) modified to account for the assumed non-volatility and irreversibility of OM_{AR}. After OM_{AR} formation, the amount of the remaining $C_{T,i}$ of each lumping group that partitions between the gas and the SHMP aerosol is calculated as a function of the effective gas-phase saturation concentration of i ($C_{g,i}^* = 1/K_{mix,i}$) using a mass balance following Eq. (10),

$$OM_{P,i} = \left[(C_{T,i} - OM_{AR,i}) - C_{g,i}^* \frac{\frac{C_{mix,i}}{MW_i}}{\sum_i \left(\frac{C_{mix,i}}{MW_i} + \frac{OM_{AR,i}}{MW_{oli,i}} \right) + OM_o} \right], \tag{12}$$

where MW_k and MW_{oli} are the molecular weight ($g\,mol^{-1}$) of the lumping species and the dimer of the lumping species, respectively, and OM_o is the pre-existing organic mass ($mol\,m^{-3}$). The system of non-linear equations are solved iteratively and the calculated $OM_{P,i}$ are summed to get the total OM_P for each Δt. Unlike when i partitions into an organic only phase ($\gamma = 1$), $\gamma_{mix,i}$ is used in calculating $C_{g,i}^*$ to account for the non-ideality of i partitioning into the SHMP aerosol (Sect. 3.2). The remaining concen-

33134

trations ($C_{T,i}$ − $OM_{AR,i}$) are passed to the next time step and combined with the newly formed $i(\Delta VOC * \alpha_{m,n})$.

4 Results and discussion

4.1 Model evaluation: SOA yield, O : C, and organosulfate formation

The ability of UNIPAR to simulate the SOA formation from isoprene photooxidation in the presence and absence of acidic inorganic seeds under low initial VOC/NO$_x$ was determined through comparison of the simulated OM$_T$ and experimental OM formation (OM$_{exp}$). All OM$_{exp}$ were corrected for particle wall loss. Figure 3 shows measured and predicted SOA formation in the presence and absence of SA at initial VOC/NO$_x$ of ∼ 17 for ISO1 and SA1 and 32 for ISO2 and SA2. In the absence of inorganic seed (ISO1 and ISO2), SOA formation is reasonably predicted by UNIPAR at both experimental conditions with a maximum SOA yield (Y_{SOA} = ΔOM_{exp}/ΔIso) of 0.025 and 0.007 for ISO1 and ISO2, respectively. These SOA yields are similar to those of reported literature values for isoprene in the absence of acidic seeds (Dommen et al., 2006). The model marginally overestimates the SOA formation in beginning of each chamber run, but the modeled OM$_T$ falls within the range of error of OM$_{exp}$ once the rate of SOA formation stabilizes and reaches a maximum.

The presence of SA seeds (shown in orange in Fig. 3) greatly increases yields under both experimental conditions resulting in Y_{SOA} of 8.5 and 4.8 % for SA1 and SA2, respectively, due to the dissolution of i into a larger M_{mix} and increased $k_{AR,i}$ attributed to the presence of [H$^+$]. Using the factor y that was fit using SA1 (Eq. 6 in Sect 3.3.1), the model accurately predicts the OM$_T$ of set SA2 in the presence of SA seed. Overall, OM$_{AR}$ is the dominant contributor to OM$_T$ for both sets contributing more than 65 and 85 % in the absence and presence of SA, respectively. Also, the higher VOC/NO$_x$ of both ISO2 and SA2 resulted in lower Y_{SOA} than ISO1 and SA1 which is discussed further in Sect. 4.3. In experiment SO2, SO$_2$ was introduced to the chamber instead of SA

seed so that the model could be further tested under a situation more representative on the ambient atmosphere in which SO_2 is oxidized to SA leading to dynamic changes in $[H^+]$ and LWC. As can be seen in Fig. 3 (shown in green), the model also reasonably predicts the OM_T.

In addition to OM_T, O : C and $[SO_4^{2-}]_{OS}$ were also predicted using the model. The predicted $[SO_4^{2-}]_{OS}$ is important due to both the formation of additional OM_{AR} and for consumption of SO_4^{2-} that leads to a reduction in $[H^+]$. In the presence of SA seed (exp. SA2), $[SO_4^{2-}]_{OS}$ was determined using the C-RUV method allowing for comparison to the model. The measured and predicted $[SO_4^{2-}]_{OS}/[SO_4^{2-}]$ were 0.32 ± 0.06 and 0.36, respectively. While the O : C of the experimental SOA were not measured, the simulated O : C can be compared to literature values which range from 0.69 to 0.88 (Bertram et al., 2011; Chen et al., 2011; Kuwata et al., 2013). UNIPAR estimates the O : C ratio using $O : C_i$ and mole fraction of each species in the aerosol phase not accounting for changes that may result from oligomerization, hydration or OS formation. In the presence of untitrated SA, the modeled O : C is 0.69 which is the lower end of the range of literature values. With increasing titration changes in composition lead to higher overall predicted O : C. In SA1, SA is partially titrated by NH_3^+ over the course of the experiment and the resulting O : C is 0.84. For ISO1 and ISO2, the O : C are 0.92 and 0.98, which is higher than the reported values. This is due to the predicted SOA being comprised of a few compounds with O : C near 1 without considering the change of molecular structures via aerosol phase reactions. Chen et al. (2011) showed a similar result in that the O : C ratio of monomeric products in isoprene SOA is higher that of oligomers.

4.2 Isoprene SOA yield and the influence of VOC/NO$_x$ and inorganic composition

In the following sections the model is used to investigate the influence of VOC/NO$_x$, LWC, and [H$^+$] on isoprene Y_{SOA} and composition. The experimental conditions of SA1 (RH, T, ΔISO) are used in all of these simulations unless otherwise specified.

Recent studies have investigated the effect of NO$_x$ on the SOA formation of isoprene for the high NO$_x$ regime (VOC/NO$_x$ < 5.5) and in the absence of NO$_x$ (Chan et al., 2010; Kroll et al., 2006; Xu et al., 2014), and found that the Y_{SOA} of isoprene is higher when formed in the absence of NO$_x$ than in the presence of high NO$_x$ concentrations. However, very little investigation has been performed on isoprene SOA formation in the low NO$_x$ regime (VOC/NO$_x$ > 5.5) of this study. To investigate the influence of the NO$_x$ level on Y_{SOA} in this range, simulations were performed in which the VOC/NO$_x$ ratio was increased incrementally from 10 to 100 with SA seeded SOA without titration and isoprene only SOA. The Y_{SOA} of each simulation are plotted in Fig. 4. Overall, with decreasing VOC/NO$_x$ (increasing NO$_x$), Y_{SOA} increases in all cases, as opposed to the high NO$_x$ regime where increases in NO$_x$ lead to a reduction in Y_{SOA} (Kroll et al., 2006). RO radicals produced from the reaction of RO$_2$ radical and NO can lead to carbonyls via reaction with oxygen, or glyoxal and methylglyoxal through fragmentation, which are highly reactive in the aerosol phase. This is illustrated by the more drastic reduction in Y_{SOA} of SA seeded SOA due to the sensitivity of these compounds to acid catalyzed reactions. Furthermore, some late generation RO$_2$ radical react with NO and form low volatile peroxynitrate (C510OOH in MCM). Therefore, increases in VOC/NO$_x$ within the simulation condition (10 ~ 100) of this study leads to increases Y_{SOA}. Figure S5 shows the stoichiometric mass coefficients ($\alpha_{m,n}$) of important products as a function of VOC/NO$_x$.

Y_{SOA} is also dynamically related to inorganic composition. SOA formation in the absence of inorganic seed is primarily a function of the characteristics of i. The impact of LWC on isoprene SOA is minimal. However, under ambient conditions SOA will typically

be formed in the presence of inorganic aerosol. Variations in the composition of the inorganic aerosol ($[SO_4^{2-}]$ and $[NH_4^+]$) and RH lead to significant changes in LWC and $[H^+]$. At high LWC, the total volume of absorptive mass (M_{mix}) increases allowing for hydrophilic i to partition into the aerosol in significant amounts and engage in aerosol

5 phase reactions. Additionally, highly reactive species such as IEPOX will react to rapidly form SOA in the presence of $[H^+]$ (Gaston et al., 2014). In Fig. 5 the simulated Y_{SOA} is plotted as a function of the fractional free sulfate (FFS), ($[SO_4^{2-}]-0.5[NH_4^+])/[SO_4^{2-}]$), and RH. The lowest Y_{SOA} occur below the ERH. For AS seeded SOA (FFS = 0.0), simulated Y_{SOA} gradually increases with increasing RH due to the rise in LWC. As FFS

10 increases (the aerosol becomes more acidic), Y_{SOA} dramatically increases at a given RH, e.g. Y_{SOA} increases from 0.033 to 0.138 when FFS changes from 0 (AS) to 1.0 (SA) at 60 % RH. At a high FFS Y_{SOA} falls with increases in RH as a result of the reduction in $[H^+]$ from the higher LWC. Therefore, Y_{SOA} of isoprene SOA is concluded to be much more sensitive to $[H^+]$ than to LWC but dynamically related to both.

15 ## 4.3 Simulated composition of isoprene SOA

Analysis of the contributions of each i to the overall OM_T allows for a determination of the species that are significant in isoprene SOA for various inorganic compositions. Four simulations were performed at 60 % RH with AS and SA seeds at org:sulf of 0.5 and 1.5 to capture the differences in composition as a result of changes in LWC, $[H^+]$,

20 and M_{mix}.

The aerosol mass fraction of each i (MF_i) under the simulated conditions are shown in Fig. 6. IEPOX has been demonstrated to be an important precursor to ambient (Budisulistiorini et al., 2015; Chan et al., 2010) and laboratory generated (Lin et al., 2012; Paulot et al., 2009) isoprene SOA leading to the formation of 2-methyltetrols (Surratt

25 et al., 2010), OS (Liao et al., 2015), and other species through aerosol phase reactions in which IEPOX products contribute up to 33 % of ambient OM in Southeast US (Budisulistiorini et al., 2013). The formation of IEPOX derived SOA has been shown to be primarily from the reactive uptake in the presence of LWC and $[H^+]$, but is most highly

correlated with aerosol acidity (Gaston et al., 2014). In Fig. 6, it can be seen that the MF_i of IEPOX derived SOA is higher in the presence of $[H^+]$. When accounting for the yield of each system, the total formation of IEPOX derived SOA is much greater in the presence of SA seed than AS seed. Additionally, the MFi of IEPOX derived SOA falls within the range measured in literature. When org : sulf increases from 0.5 to 1.5 in the presence of SA, the reduction of MF_i of IEPOX products is due to the increasing contribution of other i (7MA and OTHER) while the mass contribution of IEPOX remains similar. The MF_i of glyoxal (GLY) is significant for all four simulations, but increases with growth of M_{mix} due to its high aqueous solubility and tendency to form hydrates that can form oligomers.

In the absence of acidity, $k_{AR,i}$ are relatively small and the MF_i are primarily a function of the gas phase concentration, volatility and solubility of i. For example, in the AS seeded SOA simulations, $3OS_p$-M (products with both reactive groups and alcohols, Fig. S3) contributes more than half of the total mass (Fig. 6) due to its high gas phase concentration and low volatility. As LWC and $k_{AR,i}$ increase (AS to SA seed aerosol and org:sulf 1.5 to 0.5), more volatile and reactive i are able to contribute to MF_i. Therefore, the MF_i of $3OS_p$-M is significantly reduced in SA seeded SOA as other i contribute in larger fractions. Overall, OM_P only contributes a small fraction of the total OM_T, and the MF_i of the partitioning species generally decreases with increasing contribution of other species at higher LWC and $[H^+]$.

4.4   Model sensitivity, uncertainty, and limitations

UNIPAR utilizes the chemical structures provided by MCM to estimate the thermodynamic properties of the gas phase products, which are lumped based on their calculated vapor pressure (8 groups) and aerosol phase reactivity (6 groups). However, since not all atmospheric reactions have been studied in detail, MCM determines the products and kinetics of unstudied reactions using the known degradation mechanisms of similar chemical species. Pinho et al. (2005) evaluated the isoprene mechanism of MCM v3 by comparing the oxidation of isoprene and its products methacrolein and

methylvinyl ketone to chamber data. The model performed reasonably well for these limited products, but a large amount of uncertainty remains in regards to the prediction of the hundreds of other isoprene derived products. Furthermore, the lumping approach of UNIPAR uses a fixed gas phase composition set at the maximum HO_2/NO for each VOC/NO_x ratio. This approach does not account for changes to the gas phase composition that occur due to continued oxidation.

Deviation of the estimated $p_{L,i}^o$ from the actual $p_{L,i}^o$ due to the uncertainty of the group contribution method (Sect. 3.1) can change the lumping assignment affecting both OM_P and OM_{AR}. The uncertainty associated with the group contribution method used for $p_{L,i}^o$ estimation is a factor of 1.45 (Joback and Reid, 1987; Stein and Brown, 1994; Zhao et al., 1999). The temperature dependency of each lumping group as is calculated as a function of the enthalpy of vaporization (ΔH_{vap}) and also has associated uncertainty that can affect the model prediction. The error of this method is 2.6 % (Kolská et al., 2005). To determine the model sensitivity to these parameters, simulations of SA1 were performed by increasing and decreasing $p_{L,i}^o$ and ΔH_{vap} by a factor of 1.5 and 1.1, respectively. The change in OM_T from the baseline for each simulation is shown in Fig. S6. Increasing and decreasing $p_{L,i}^o$ by a factor of 1.5 results in a 32.03 and −26.41 % change, respectively, while modifying ΔH_{vap} only leads to ±0.27 % change.

The thermodynamic model AIOMFAC was employed to generate a simplified parameterization to estimate $\gamma_{mix,i}$ in the SHMP isoprene SOA as a function of O : C, org:sulf, RH, and V_{mol}. AIOMFAC is a valuable tool for predicting the activity coefficients of complex mixtures, but it has substantial uncertainty resulting from limitations of the database used in development and the error associated with the underlying modules. Moreover, the expected accuracy is limited further by the regression performed in UNIPAR. For the condition simulated by UNIPAR, $\gamma_{mix,i}$ are all near unity (0.65–1.75). Considering the characteristics of a SHMP aerosol, a factor of 1.5 was applied to the predicted $\gamma_{mix,i}$ and the resulting change in OM_T is −16.22 %/+32.00 % (Fig. S6), which is similar to the model sensitivity to $p_{L,i}^o$.

The other parameter largely affecting the simulated SOA formation in UNIPAR is $k_{AR,i}$, which is calculated primarily as a function of LWC, [H$^+$], and reactivity of i (Sect. 3.3.1). Estimations of LWC and [H$^+$] are performed by the inorganic thermodynamic model E-AIM. Similar to AIOMFAC, the accuracy of E-AIM will depend on the underlying assumptions and the database used in development. For LWC, the predictions of E-AIM are consistent with other inorganic thermodynamic models and are based on widely used, critically reviewed water activity data (Zhang et al., 2000). However, inorganic thermodynamic models vary widely in predicting [H$^+$] especially at low RH. This is especially true for ammonia rich inorganic salts at low RH. Corrections for the ammonia rich predictions of [H$^+$] were applied based on the results of Li and Jang (2012) in which aerosol [H$^+$] was measured using a filter based colorimetry method coupled with a PILS-IC. The total uncertainty of this method is approximately 18 %. There is also uncertainty stemming from the flow chamber study that was used to fit the coefficients used in predicting $k_{AR,i}$. To determine the possible sensitivity of the model to the combined uncertainty of the corrected E-AIM and the function used to predict $k_{AR,i}$, a factor of 2.0 was applied to simulations and the resulting change in OM$_T$ is approximately ±13 % (Fig. S6).

Furthermore, not all recent advancements in the understanding of SOA formation mechanisms are accounted for by UNIPAR, including but not limited to SOA viscosity, nighttime chemistry of nitrate radicals (NO$_3^*$), and SVOC wall loss. Virtanen et al. (2010) reported that biogenic SOA can exist as amorphous solids or glassy state, which can lead to deviations from equilibrium processes, but Song et al. (2015) found that isoprene derived SOA is of low viscosity under the range of ambient RH. Thus, impact of viscosity on isoprene SOA is minimal. The nighttime reaction of isoprene with NO$_3^*$ has been found to lead to significant SOA formation due to the formation of stable primary organonitrate (ON). Ng et al. (2008) measured SOA yields up to 23.8 % from the dark chamber reaction of isoprene and NO$_3^*$ under dry conditions (< 10 % RH), while Rollins et al. (2012) linked NO$_3^*$ chemistry to ambient, nighttime SOA production with 27 to 40 % of nighttime OM growth from ON. Under low NO$_x$ conditions, isoprene photoox-

Simulating isoprene SOA formation in the presence of inorganics

R. L. Beardsley and M. Jang

Title Page

Abstract	Introduction
Conclusions	References
Tables	Figures

|◄ | ►|

◄ | ►

Back | Close

Full Screen / Esc

Printer-friendly Version

Interactive Discussion

idation has been shown to produce primarily tertiary ON in both the gas phase and through aerosol phase epoxide reactions (Eddingsaas et al., 2010; Paulot et al., 2009). Darer et al. (2011) investigated the stability of primary and tertiary ON and found the tertiary ON to be highly unstable and to rapidly convert to OS and polyols in both neutral and acidic SOA. Therefore, it is unlikely that ON significantly contribute to the SOA investigated and modeled in this study.

In the recent Southern Oxidant and Aerosol Study field campaign, Budisulistiorini et al. (2015) and Xu et al. (2015) found ambient isoprene SOA formation in the SE US to be most highly correlated with $[SO_4^{2-}]$, and insensitive to $[H^+]$ and LWC. However, in the summer months the aerosol of the SE US are highly acidic (pH 0 to 2) and high in LWC due to the high RH ($> 50\,\%$). Under these conditions, the formation of isoprene derived SOA is not likely to be highly correlated with changes in LWC and $[H^+]$ since both are always high. Yet when comparing neutral and acidic conditions, the presence of acidity has repeatedly been shown to lead to increases in Y_{SOA} (Lin et al., 2012; Surratt et al., 2007). Most recently, Lewandowski et al. (2015) found up to a 459 % increase in Y_{SOA} from the presence of $[H^+]$. Additionally, Xu et al. (2015) found a reduction in isoprene derived SOA with increases in RH for the highly acidic aerosol of the study. A similar reduction with increasing RH is seen at high FFS in Fig. 5 due to the dilution of SO_4^{2-} and the corresponding $[H^+]$ by increases in LWC.

5   Conclusions and atmospheric implications

Under the assumption of SHMP aerosol, UNIPAR was able to simulate the low NO_x SOA formation of isoprene from partitioning and aerosol phase reactions with and without an inorganic acid seed. The data used to validate the model was generated using the UF-APHOR outdoor chamber, which allows for day long experiments under ambient sunlight, T and RH. For the SOA formation of isoprene in the absence of deliquesced inorganic seeds, UNIPAR was able to predict the experimental OM_T using the same approach that was applied to anthropogenic, aromatic VOCs in Im et al. (2014)

without any modification. Differences between the SHMP SOA formed by isoprene in the presence of deliquesced inorganic seeds and LLPS SOA of the previous study required a slight reduction in $k_{AR,i}$. After validating the model using the measured SOA formation of outdoor chamber experiments, simulations were performed to elucidate the sensitivity of Y_{SOA} and composition to model parameters. From this analysis it was determined that the Y_{SOA} of isoprene and the resulting SOA composition is primarily a function of VOC/NO$_x$, [H$^+$], and LWC. For the range of VOC/NO$_x$ investigated in this study ($\geq$ 10), increases in NO$_x$ corresponded with increases in Y_{SOA} and a higher sensitivity to [H$^+$]. This is due to the increased production of highly reactive carbonyls, such as glyoxal, and a more general shift to lower volatility (Fig. S6).

Changes in [H$^+$] and LWC were shown to strongly influence Y_{SOA} (Fig. 5). At a given RH, increases in [H$^+$] result in increased OM formation. For titrated acidic aerosol, increases in RH lead to gradual increases in Y_{SOA}. However for highly acidic aerosol (FFS $\geq$ 0.75), increases in RH decrease Y_{SOA} due to dilution of [H$^+$]. Overall, isoprene SOA formation was found to be most sensitive to [H$^+$] with the highest Y_{SOA} occurring at high FFS and low RH.

Due to the pervasiveness of isoprene in the ambient atmosphere, any variation in Y_{SOA} will have a strong influence on the global SOA budget and needs to be accounted for by climate and air quality models. Since the experimental runs and simulations performed in this study were at concentrations beyond those of the ambient atmosphere, additional simulations were performed to estimate Y_{SOA} for conditions more representative of the ambient atmosphere. The ΔISO during each Δt was assumed to be constant and estimated assuming a pseudo first order reaction with OH using an isoprene concentration of 2.4 ppb from the rural measurements of Wiedinmyer et al. (2001) and a OH concentration of 1.0×10^{-6} molecules cm^{-3}. Using a [SO$_4^{2-}$] of 5.55 μg m^{-3} and OM$_o$ of 3 μg m^{-3} based on the non-urban continental composition of submicron PM from the review of Heintzenberg (1989), two sets of simulations were performed for AS and AHS at RH of 30 and 60 % and VOC/NO$_x$ = 10. The simulated Y_{SOA} of AS are 0.01695 (OM$_T$ = 0.329 μg m^{-3}) and 0.0207 (OM$_T$ = 0.402 μg m^{-3}), and of AHS are

R. L. Beardsley and M. Jang

Title Page

Abstract | Introduction

Conclusions | References

Tables | Figures

|◄ | ►|

◄ | ►

Back | Close

Full Screen / Esc

Printer-friendly Version

Interactive Discussion

0.0446 (OM_T = 0.867 µg m^{-3}) and 0.0449 (OM_T = 0.873 µg m^{-3}) at 30 and 60 % RH, respectively. The OM_T formation and associated Y_{SOA} were calculated after an eight hour simulation. AS at 30 % RH is the seen as the baseline as it is below the ERH. Increasing the RH to 60 % leads to a 22 % increase in Y_{SOA} for AS due to the increased LWC.

5 The presence of AHS seeds and the resultant increase in [H$^+$] leads to an increase of 163 and 165 % in Y_{SOA} over the baseline at 30 and 60 % RH, respectively. These results support the conclusion that the SOA formation of isoprene is more sensitive to [H$^+$] than to LWC, but dynamically related to both. Furthermore, while the SOA formation of isoprene may be reasonably predicted as a linear function of [H$^+$] for a specific

10 RH and VOC/NO$_x$, as is proposed by Surratt et al. (2007), a single linear relationship will not hold at different RH for a single VOC/NO$_x$ or under the possible range of conditions in the ambient atmosphere. In the application of UNIPAR to the aromatic LLPS SOA system, Im et al. (2014) found the Y_{SOA} of toluene to be higher in the presence AHS than AS at 30 % RH, but the same at 60 % RH meaning that the SOA forma-

15 tion of toluene is less sensitive to [H$^+$] but more sensitive to LWC than isoprene. The relationship between Y_{SOA}, LWC, and [H$^+$] will not only vary dynamically for different VOC/NO$_x$ but also between different VOC systems. Failure to account for these relationships in regional and global scale models may lead to significant underestimation of SOA formation in acidic and humid conditions.

20 **The Supplement related to this article is available online at doi:10.5194/acpd-15-33121-2015-supplement.**

Title Page

Abstract | Introduction

Conclusions | References

Tables | Figures

|◄ | ►|

◄ | ►

Back | Close

Full Screen / Esc

Printer-friendly Version

Interactive Discussion

References

Aiken, A. C., DeCarlo, P. F., Kroll, J. H., Worsnop, D. R., Huffman, J. A., Docherty, K. S., Ulbrich, I. M., Mohr, C., Kimmel, J. R., Sueper, D., Sun, Y., Zhang, Q., Trimborn, A., Northway, M., Ziemann, P. J., Canagaratna, M. R., Onasch, T. B., Alfarra, M. R., Prevot, A. S. H., Dommen, J., Duplissy, J., Metzger, A., Baltensperger, U., and Jimenez, J. L.: O / C and OM / OC ratios of primary, secondary, and ambient organic aerosols with high-resolution time-of-flight aerosol mass spectrometry, Environ. Sci. Technol., 42, 4478–4485, doi:10.1021/es703009q, 2008.

Bertram, A. K., Martin, S. T., Hanna, S. J., Smith, M. L., Bodsworth, A., Chen, Q., Kuwata, M., Liu, A., You, Y., and Zorn, S. R.: Predicting the relative humidities of liquid-liquid phase separation, efflorescence, and deliquescence of mixed particles of ammonium sulfate, organic material, and water using the organic-to-sulfate mass ratio of the particle and the oxygen-to-carbon elemental ratio of the organic component, Atmos. Chem. Phys., 11, 10995–11006, doi:10.5194/acp-11-10995-2011, 2011.

Budisulistiorini, S. H., Canagaratna, M. R., Croteau, P. L., Marth, W. J., Baumann, K., Edgerton, E. S., Shaw, S. L., Knipping, E. M., Worsnop, D. R., Jayne, J. T., Gold, A., and Surratt, J. D.: Real-time continuous characterization of secondary organic aerosol derived from isoprene epoxydiols in downtown Atlanta, Georgia, using the aerodyne aerosol chemical speciation monitor, Environ. Sci. Technol., 47, 5686–5694, doi:10.1021/es400023n, 2013.

Budisulistiorini, S. H., Li, X., Bairai, S. T., Renfro, J., Liu, Y., Liu, Y. J., McKinney, K. A., Martin, S. T., McNeill, V. F., Pye, H. O. T., Nenes, A., Neff, M. E., Stone, E. A., Mueller, S., Knote, C., Shaw, S. L., Zhang, Z., Gold, A., and Surratt, J. D.: Examining the effects of anthropogenic emissions on isoprene-derived secondary organic aerosol formation during the 2013 Southern Oxidant and Aerosol Study (SOAS) at the Look Rock, Tennessee ground site, Atmos. Chem. Phys., 15, 8871–8888, doi:10.5194/acp-15-8871-2015, 2015.

Carlton, A. G., Wiedinmyer, C., and Kroll, J. H.: A review of Secondary Organic Aerosol (SOA) formation from isoprene, Atmos. Chem. Phys., 9, 4987–5005, doi:10.5194/acp-9-4987-2009, 2009.

Chan, M. N., Surratt, J. D., Claeys, M., Edgerton, E. S., Tanner, R. L., Shaw, S. L., Zheng, M., Knipping, E. M., Eddingsaas, N. C., Wennberg, P. O., and Seinfeld, J. H.: Characterization and quantification of isoprene-derived epoxydiols in ambient aerosol in the southeastern United States, Environ. Sci. Technol., 44, 4590–4596, doi:10.1021/es100596b, 2010.

Chen, Q., Liu, Y., Donahue, N. M., Shilling, J. E., and Martin, S. T.: Particle-phase chemistry of secondary organic material: modeled compared to measured $O:C$ and $H:C$ elemental ratios provide constraints, Environ. Sci. Technol., 45, 4763–4770, doi:10.1021/es104398s, 2011.

Claeys, M., Wang, W., Ion, A. C., Kourtchev, I., Gelencsér, A., and Maenhaut, W.: Formation of secondary organic aerosols from isoprene and its gas-phase oxidation products through reaction with hydrogen peroxide, Atmos. Environ., 38, 4093–4098, doi:10.1016/j.atmosenv.2004.06.001, 2004.

Clegg, S. L., Brimblecombe, P., and Wexler, A. S.: Thermodynamic model of the system H^+-NH_4^+-SO_4^{2-}-NO_3^--H_2O at tropospheric temperatures, J. Phys. Chem. A, 102, 2137–2154, doi:10.1021/jp973042r, 1998.

Darer, A. I., Cole-Filipiak, N. C., O'Connor, A. E., and Elrod, M. J.: Formation and stability of atmospherically relevant isoprene-derived organosulfates and organonitrates, Environ. Sci. Technol., 45, 1895–1902, doi:10.1021/es103797z, 2011.

Dommen, J., Metzger, A., Duplissy, J., Kalberer, M., Alfarra, M. R., Gascho, A., Weingartner, E., Prevot, A. S. H., Verheggen, B., and Baltensperger, U.: Laboratory observation of oligomers in the aerosol from isoprene / NO_x photooxidation, Geophys. Res. Lett., 33, L13805, doi:10.1029/2006GL026523, 2006.

Eddingsaas, N. C., VanderVelde, D. G., and Wennberg, P. O.: Kinetics and products of the acid-catalyzed ring-opening of atmospherically relevant butyl epoxy alcohols, J. Phys. Chem. A, 114, 8106–8113, doi:10.1021/jp103907c, 2010.

Edney, E. O., Kleindienst, T. E., Jaoui, M., Lewandowski, M., Offenberg, J. H., Wang, W., and Claeys, M.: Formation of 2-methyl tetrols and 2-methylglyceric acid in secondary organic aerosol from laboratory irradiated isoprene/NO_x/SO_2/air mixtures and their detection in ambient $PM_{2.5}$ samples collected in the eastern United States, Atmos. Environ., 39, 5281–5289, doi:10.1016/j.atmosenv.2005.05.031, 2005.

Gaston, C. J., Riedel, T. P., Zhang, Z., Gold, A., Surratt, J. D., and Thornton, J. A.: Reactive uptake of an isoprene-derived epoxydiol to submicron aerosol particles, Environ. Sci. Technol., 48, 11178–11186, doi:10.1021/es5034266, 2014.

Guenther, A., Karl, T., Harley, P., Wiedinmyer, C., Palmer, P. I., and Geron, C.: Estimates of global terrestrial isoprene emissions using MEGAN (Model of Emissions of Gases and Aerosols from Nature), Atmos. Chem. Phys., 6, 3181–3210, doi:10.5194/acp-6-3181-2006, 2006.

Simulating isoprene SOA formation in the presence of inorganics

R. L. Beardsley and M. Jang

Title Page

Abstract | Introduction

Conclusions | References

Tables | Figures

|◄ | ►|

◄ | ►

Back | Close

Full Screen / Esc

Printer-friendly Version

Interactive Discussion

Heintzenberg, J.: Fine particles in the global troposphere a review, Tellus B, 41, 149–160, doi:10.1111/j.1600-0889.1989.tb00132.x, 1989.

Hennigan, C. J., Bergin, M. H., Dibb, J. E., and Weber, R. J.: Enhanced secondary organic aerosol formation due to water uptake by fine particles, Geophys. Res. Lett., 35, L18801, doi:10.1029/2008GL035046, 2008.

Henze, D. K. and Seinfeld, J. H.: Global secondary organic aerosol from isoprene oxidation, Geophys. Res. Lett., 33, L09812, doi:10.1029/2006GL025976, 2006.

Hodas, N., Zuend, A., Mui, W., Flagan, R. C., and Seinfeld, J. H.: Influence of particle-phase state on the hygroscopic behavior of mixed organic–inorganic aerosols, Atmos. Chem. Phys., 15, 5027–5045, doi:10.5194/acp-15-5027-2015, 2015.

Im, Y., Jang, M., and Beardsley, R. L.: Simulation of aromatic SOA formation using the lumping model integrated with explicit gas-phase kinetic mechanisms and aerosol-phase reactions, Atmos. Chem. Phys., 14, 4013–4027, doi:10.5194/acp-14-4013-2014, 2014.

Ip, H. S. S., Huang, X. H. H., and Yu, J. Z.: Effective Henry's law constants of glyoxal, glyoxylic acid, and glycolic acid, Geophys. Res. Lett., 36, L01802, doi:10.1029/2008GL036212, 2009.

Jang, M. and Kamens, R. M.: A thermodynamic approach for modeling partitioning of semivolatile organic compounds on atmospheric particulate matter: humidity effects, Environ. Sci. Technol., 32, 1237–1243, doi:10.1021/es970773w, 1998.

Jang, M., Czoschke, N. M., Lee, S., and Kamens, R. M.: Heterogeneous atmospheric aerosol production by acid-catalyzed particle-phase reactions, Science, 298, 814–817, doi:10.1126/science.1075798, 2002.

Jang, M., Carroll, B., Chandramouli, B., and Kamens, R. M.: Particle growth by acid-catalyzed heterogeneous reactions of organic carbonyls on preexisting aerosols, Environ. Sci. Technol., 37, 3828–3837, doi:10.1021/es021005u, 2003.

Jang, M., Czoschke, N. M., and Northcross, A. L.: Semiempirical model for organic aerosol growth by acid-catalyzed heterogeneous reactions of organic carbonyls, Environ. Sci. Technol., 39, 164–174, doi:10.1021/es048977h, 2005.

Jang, M., Czoschke, N. M., Northcross, A. L., Cao, G., and Shaof, D.: SOA formation from partitioning and heterogeneous reactions: model study in the presence of inorganic species, Environ. Sci. Technol., 40, 3013–3022, doi:10.1021/es0511220, 2006.

Jang, M., Cao, G., and Paul, J.: Colorimetric particle acidity analysis of secondary organic aerosol coating on submicron acidic aerosols, Aerosol Sci. Tech., 42, 409–420, doi:10.1080/02786820802154861, 2008.

Jeffries, H. E., Gary, M. W., Kessler, M., and Sexton, K. G.: Morphecule reaction mechanism, MORPHO, ALLOMORPHIC simulation software, 1998.

Joback, K. G. and Reid, R. C.: Estimation of pure-component properties from group-contributions, Chem. Eng. Commun., 57, 233–243, doi:10.1080/00986448708960487, 1987.

Kleindienst, T. E., Jaoui, M., Lewandowski, M., Offenberg, J. H., Lewis, C. W., Bhave, P. V., and Edney, E. O.: Estimates of the contributions of biogenic and anthropogenic hydrocarbons to secondary organic aerosol at a southeastern US location, Atmos. Environ., 41, 8288–8300, doi:10.1016/j.atmosenv.2007.06.045, 2007.

Kolská, Z., Růžička, V., and Gani, R.: Estimation of the enthalpy of vaporization and the entropy of vaporization for pure organic compounds at 298.15 K and at normal boiling temperature by a group contribution method, Ind. Eng. Chem. Res., 44, 8436–8454, doi:10.1021/ie050113x, 2005.

Kroll, J. H., Ng, N. L., Murphy, S. M., Flagan, R. C., and Seinfeld, J. H.: Secondary organic aerosol formation from isoprene photooxidation under high-NO_x conditions, Geophys. Res. Lett., 32, L18808, doi:10.1029/2005GL023637, 2005.

Kroll, J. H., Ng, N. L., Murphy, S. M., Flagan, R. C., and Seinfeld, J. H.: Secondary organic aerosol formation from isoprene photooxidation, Environ. Sci. Technol., 40, 1869–1877, doi:10.1021/es0524301, 2006.

Kuwata, M., Shao, W., Lebouteiller, R., and Martin, S. T.: Classifying organic materials by oxygen-to-carbon elemental ratio to predict the activation regime of Cloud Condensation Nuclei (CCN), Atmos. Chem. Phys., 13, 5309–5324, doi:10.5194/acp-13-5309-2013, 2013.

Kuwata, M., Liu, Y., McKinney, K., and Martin, S. T.: Physical state and acidity of inorganic sulfate can regulate the production of secondary organic material from isoprene photooxidation products, Phys. Chem. Chem. Phys., 17, 5670–5678, doi:10.1039/C4CP04942J, 2015.

Lewandowski, M., Jaoui, M., Offenberg, J. H., Krug, J. D., and Kleindienst, T. E.: Atmospheric oxidation of isoprene and 1,3-butadiene: influence of aerosol acidity and relative humidity on secondary organic aerosol, Atmos. Chem. Phys., 15, 3773–3783, doi:10.5194/acp-15-3773-2015, 2015.

Li, J. and Jang, M.: Aerosol acidity measurement using colorimetry coupled with a reflectance UV-visible spectrometer, Aerosol Sci. Tech., 46, 833–842, doi:10.1080/02786826.2012.669873, 2012.

Li, J., Jang, M., and Beardsley, R. L.: Dialkylsulfate formation in sulfuric acid-seeded secondary organic aerosol produced using an outdoor chamber under natural sunlight, Environ. Chem., doi:10.1071/EN15129, online first, 2015.

Liao, J., Froyd, K. D., Murphy, D. M., Keutsch, F. N., Yu, G., Wennberg, P. O., St. Clair, J. M., Crounse, J. D., Wisthaler, A., Mikoviny, T., Jimenez, J. L., Campuzano-Jost, P., Day, D. A., Hu, W., Ryerson, T. B., Pollack, I. B., Peischl, J., Anderson, B. E., Ziemba, L. D., Blake, D. R., Meinardi, S., and Diskin, G.: Airborne measurements of organosulfates over the continental US, J. Geophys. Res.-Atmos., 120, 2014JD022378, doi:10.1002/2014JD022378, 2015.

Liggio, J., Li, S.-M., and McLaren, R.: Heterogeneous reactions of glyoxal on particulate matter: identification of acetals and sulfate esters, Environ. Sci. Technol., 39, 1532–1541, doi:10.1021/es048375y, 2005.

Lim, Y. B., Tan, Y., Perri, M. J., Seitzinger, S. P., and Turpin, B. J.: Aqueous chemistry and its role in secondary organic aerosol (SOA) formation, Atmos. Chem. Phys., 10, 10521–10539, doi:10.5194/acp-10-10521-2010, 2010.

Limbeck, A., Kulmala, M., and Puxbaum, H.: Secondary organic aerosol formation in the atmosphere via heterogeneous reaction of gaseous isoprene on acidic particles, Geophys. Res. Lett., 30, 1996, doi:10.1029/2003GL017738, 2003.

Lin, Y.-H., Zhang, Z., Docherty, K. S., Zhang, H., Budisulistiorini, S. H., Rubitschun, C. L., Shaw, S. L., Knipping, E. M., Edgerton, E. S., Kleindienst, T. E., Gold, A., and Surratt, J. D.: Isoprene epoxydiols as precursors to secondary organic aerosol formation: acid-catalyzed reactive uptake studies with authentic compounds, Environ. Sci. Technol., 46, 250–258, doi:10.1021/es202554c, 2012.

Minerath, E. C., Casale, M. T., and Elrod, M. J.: Kinetics feasibility study of alcohol sulfate esterification reactions in tropospheric aerosols, Environ. Sci. Technol., 42, 4410–4415, doi:10.1021/es8004333, 2008.

Murphy, D. M., Cziczo, D. J., Froyd, K. D., Hudson, P. K., Matthew, B. M., Middlebrook, A. M., Peltier, R. E., Sullivan, A., Thomson, D. S., and Weber, R. J.: Single-particle mass spectrometry of tropospheric aerosol particles, J. Geophys. Res.-Atmos., 111, D23S32, doi:10.1029/2006JD007340, 2006.

Ng, N. L., Kwan, A. J., Surratt, J. D., Chan, A. W. H., Chhabra, P. S., Sorooshian, A., Pye, H. O. T., Crounse, J. D., Wennberg, P. O., Flagan, R. C., and Seinfeld, J. H.: Secondary organic aerosol (SOA) formation from reaction of isoprene with nitrate radicals (NO$_3$), Atmos. Chem. Phys., 8, 4117–4140, doi:10.5194/acp-8-4117-2008, 2008.

Nguyen, T. B., Roach, P. J., Laskin, J., Laskin, A., and Nizkorodov, S. A.: Effect of humidity on the composition of isoprene photooxidation secondary organic aerosol, Atmos. Chem. Phys., 11, 6931–6944, doi:10.5194/acp-11-6931-2011, 2011.

Odum, J. R., Hoffman, T., Bowman, F., Collins, D., Flagan, R. C., and Seinfeld, J. H.: Gas/particle partitioning and secondary organic aerosol yields, Environ. Sci. Technol., 30, 2580–2585, 1996.

Pandis, S. N., Paulson, S. E., Seinfeld, J. H., and Flagan, R. C.: Aerosol formation in the photooxidation of isoprene and β-pinene, Atmos. Environ. A Gen., 25, 997–1008, doi:10.1016/0960-1686(91)90141-S, 1991.

Pankow, J. F.: An absorption model of gas/particle partitioning of organic compounds in the atmosphere, Atmos. Environ., 28, 185–188, doi:10.1016/1352-2310(94)90093-0, 1994.

Paulot, F., Crounse, J. D., Kjaergaard, H. G., Kürten, A., Clair, J. M. S., Seinfeld, J. H., and Wennberg, P. O.: Unexpected epoxide formation in the gas-phase photooxidation of isoprene, Science, 325, 730–733, doi:10.1126/science.1172910, 2009.

Pinho, P. G., Pio, C. A., and Jenkin, M. E.: Evaluation of isoprene degradation in the detailed tropospheric chemical mechanism, MCM v3, using environmental chamber data, Atmos. Environ., 39, 1303–1322, doi:10.1016/j.atmosenv.2004.11.014, 2005.

Kamens, R. M., Gery, M. W., Jeffries, H. E., Jackson, M., and Cole, E. I.: Ozone-isoprene reactions: Product formation and aerosol potential, Int. J. Chem. Kinet., 14, 955–975, doi:10.1002/kin.550140902, 1982.

Rollins, A. W., Browne, E. C., Min, K.-E., Pusede, S. E., Wooldridge, P. J., Gentner, D. R., Goldstein, A. H., Liu, S., Day, D. A., Russell, L. M., and Cohen, R. C.: Evidence for NO$_x$ control over nighttime SOA formation, Science, 337, 1210–1212, doi:10.1126/science.1221520, 2012.

Saunders, S. M., Jenkin, M. E., Derwent, R. G., and Pilling, M. J.: World wide web site of a master chemical mechanism (MCM) for use in tropospheric chemistry models, Atmos. Environ., 31, 1249–1249, doi:10.1016/S1352-2310(97)85197-7, 1997.

Saunders, S. M., Jenkin, M. E., Derwent, R. G., and Pilling, M. J.: Protocol for the development of the Master Chemical Mechanism, MCM v3 (Part A): tropospheric degradation of non-aromatic volatile organic compounds, Atmos. Chem. Phys., 3, 161–180, doi:10.5194/acp-3-161-2003, 2003.

Title Page

Abstract | Introduction

Conclusions | References

Tables | Figures

|◄ | ►|

◄ | ►

Back | Close

Full Screen / Esc

Printer-friendly Version

Interactive Discussion

Schell, B., Ackermann, I. J., Hass, H., Binkowski, F. S., and Ebel, A.: Modeling the formation of secondary organic aerosol within a comprehensive air quality model system, J. Geophys. Res.-Atmos., 106, 28275–28293, doi:10.1029/2001JD000384, 2001.

Song, M., Liu, P. F., Hanna, S. J., Li, Y. J., Martin, S. T., and Bertram, A. K.: Relative humidity-dependent viscosities of isoprene-derived secondary organic material and atmospheric implications for isoprene-dominant forests, Atmos. Chem. Phys., 15, 5145–5159, doi:10.5194/acp-15-5145-2015, 2015.

Stein, S. E. and Brown, R. L.: Estimation of normal boiling points from group contributions, J. Chem. Inf. Model., 34, 581–587, doi:10.1021/ci00019a016, 1994.

Surratt, J. D., Lewandowski, M., Offenberg, J. H., Jaoui, M., Kleindienst, T. E., Edney, E. O., and Seinfeld, J. H.: Effect of acidity on secondary organic aerosol formation from isoprene, Environ. Sci. Technol., 41, 5363–5369, doi:10.1021/es0704176, 2007.

Surratt, J. D., Chan, A. W. H., Eddingsaas, N. C., Chan, M., Loza, C. L., Kwan, A. J., Hersey, S. P., Flagan, R. C., Wennberg, P. O., and Seinfeld, J. H.: Reactive intermediates revealed in secondary organic aerosol formation from isoprene, P. Natl. Acad. Sci. USA, 107, 6640–6645, doi:10.1073/pnas.0911114107, 2010.

Virtanen, A., Joutsensaari, J., Koop, T., Kannosto, J., Yli-Pirilä, P., Leskinen, J., Mäkelä, J. M., Holopainen, J. K., Pöschl, U., Kulmala, M., Worsnop, D. R., and Laaksonen, A.: An amorphous solid state of biogenic secondary organic aerosol particles, Nature, 467, 824–827, doi:10.1038/nature09455, 2010.

Volkamer, R., San Martini, F., Molina, L. T., Salcedo, D., Jimenez, J. L., and Molina, M. J.: A missing sink for gas-phase glyoxal in Mexico City: formation of secondary organic aerosol, Geophys. Res. Lett., 34, L19807, doi:10.1029/2007GL030752, 2007.

Volkamer, R., Ziemann, P. J., and Molina, M. J.: Secondary Organic Aerosol Formation from Acetylene (C_2H_2): seed effect on SOA yields due to organic photochemistry in the aerosol aqueous phase, Atmos. Chem. Phys., 9, 1907–1928, doi:10.5194/acp-9-1907-2009, 2009.

Wiedinmyer, C., Friedfeld, S., Baugh, W., Greenberg, J., Guenther, A., Fraser, M., and Allen, D.: Measurement and analysis of atmospheric concentrations of isoprene and its reaction products in central Texas, Atmos. Environ., 35, 1001–1013, doi:10.1016/S1352-2310(00)00406-4, 2001.

Xu, L., Kollman, M. S., Song, C., Shilling, J. E., and Ng, N. L.: Effects of NO_x on the volatility of secondary organic aerosol from isoprene photooxidation, Environ. Sci. Technol., 48, 2253–2262, doi:10.1021/es404842g, 2014.

Title Page

Abstract · Introduction

Conclusions · References

Tables · Figures

|◄ · ►|

◄ · ►

Back · Close

Full Screen / Esc

Printer-friendly Version

Interactive Discussion

Xu, L., Guo, H., Boyd, C. M., Klein, M., Bougiatioti, A., Cerully, K. M., Hite, J. R., Isaacman-VanWertz, G., Kreisberg, N. M., Knote, C., Olson, K., Koss, A., Goldstein, A. H., Hering, S. V., Gouw, J. de, Baumann, K., Lee, S.-H., Nenes, A., Weber, R. J., and Ng, N. L.: Effects of anthropogenic emissions on aerosol formation from isoprene and monoterpenes in the southeastern United States, P. Natl. Acad. Sci. USA, 112, 37–42, doi:10.1073/pnas.1417609112, 2015.

Zhang, H., Worton, D. R., Lewandowski, M., Ortega, J., Rubitschun, C. L., Park, J.-H., Kristensen, K., Campuzano-Jost, P., Day, D. A., Jimenez, J. L., Jaoui, M., Offenberg, J. H., Kleindienst, T. E., Gilman, J., Kuster, W. C., de Gouw, J., Park, C., Schade, G. W., Frossard, A. A., Russell, L., Kaser, L., Jud, W., Hansel, A., Cappellin, L., Karl, T., Glasius, M., Guenther, A., Goldstein, A. H., Seinfeld, J. H., Gold, A., Kamens, R. M., and Surratt, J. D.: Organosulfates as tracers for Secondary Organic Aerosol (SOA) formation from 2-Methyl-3-Buten-2-ol (MBO) in the atmosphere, Environ. Sci. Technol., 46, 9437–9446, doi:10.1021/es301648z, 2012.

Zhang, Y., Seigneur, C., Seinfeld, J. H., Jacobson, M., Clegg, S. L., and Binkowski, F. S.: A comparative review of inorganic aerosol thermodynamic equilibrium modules: similarities, differences, and their likely causes, Atmos. Environ., 34, 117–137, doi:10.1016/S1352-2310(99)00236-8, 2000.

Zhao, L., Li, P., and Yalkowsky, S. H.: Predicting the entropy of boiling for organic compounds, J. Chem. Inf. Model., 39, 1112–1116, doi:10.1021/ci990054w, 1999.

Title Page

Abstract | Introduction

Conclusions | References

Tables | Figures

|◄ | ►|

◄ | ►

Back | Close

Full Screen / Esc

Printer-friendly Version

Interactive Discussion

Simulating isoprene SOA formation in the presence of inorganics
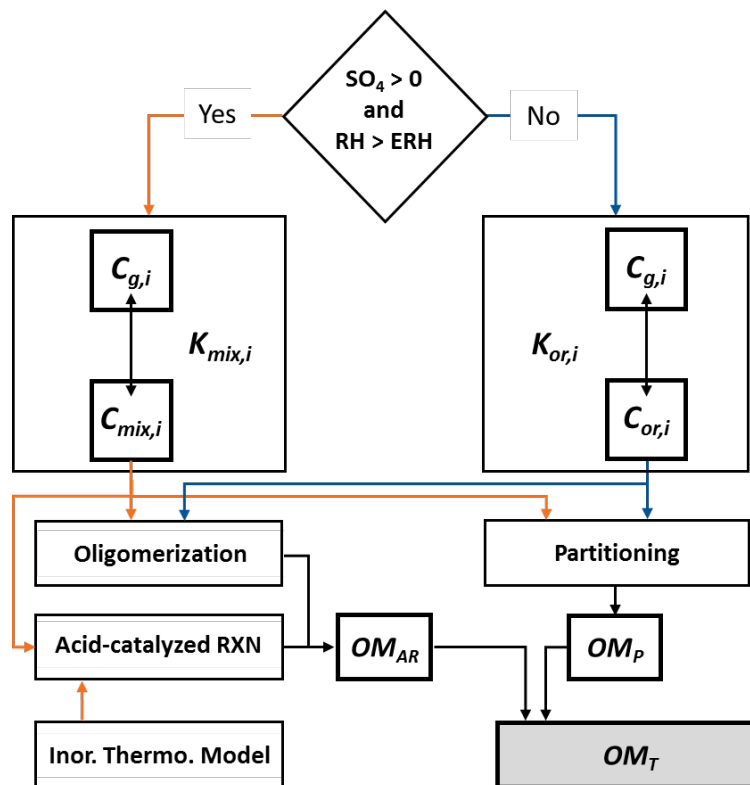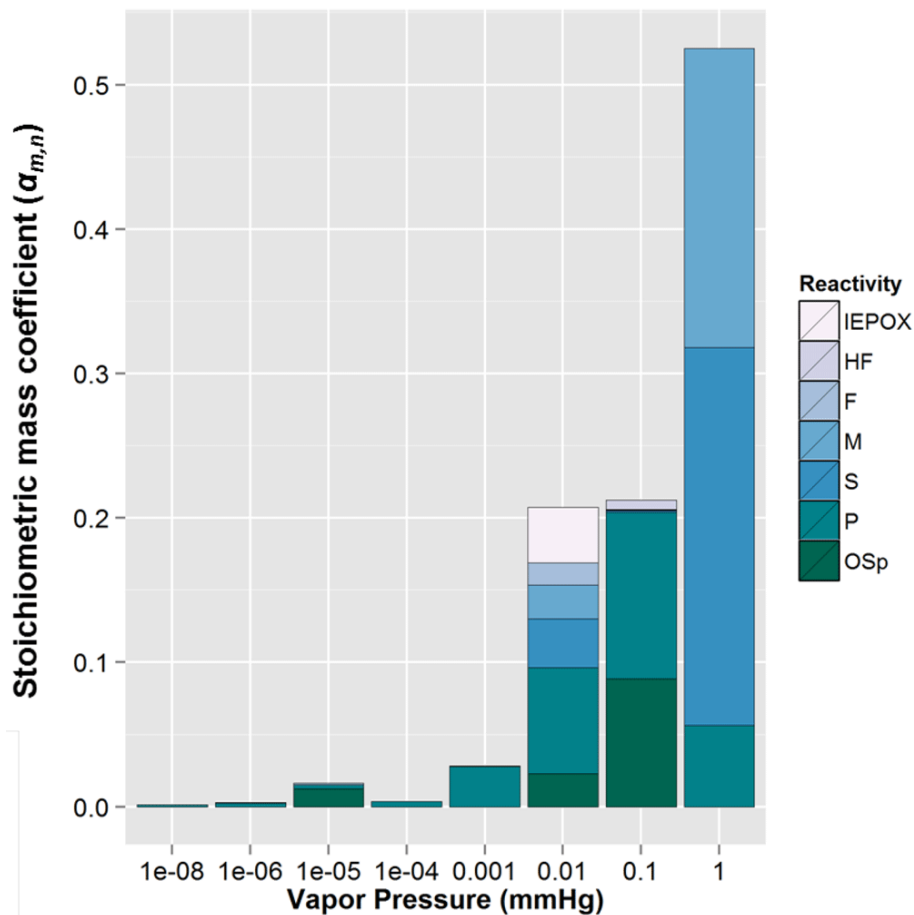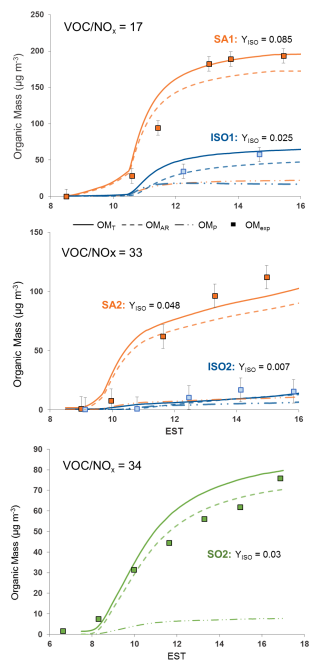
R. L. Beardsley and M. Jang

Table 1. Experimental conditions and resulting SOA data of the isoprene photooxidation experiments performed with and without inorganic acidic seed in the dual, outdoor UF APHOR chambers.

Exp.	Date	RH (%)	Temp (K)	$[\text{ISO}]_0$ (ppb)	$[\text{NO}_x]_0$ (ppb)	VOC/NO_x (ppbC ppb^{-1})	$[\text{H}_2\text{SO}_4]$ (µg m^{-3})	$Y_{\text{SOA}}^{\text{a}}$ (%)
ISO1	27 Jan 2015	27–66	279–298	839	241	17.4	0	2.5
SA1	27 Jan 2015	20–54	279–299	850	253	16.8	53	8.5
ISO2	14 Dec 2014	19–49	282–303	852	131	32.7	0	0.7
SA2	14 Dec 2014	14–40	284–305	857	130	32.5	40	4.8
SO2	18 Jan 2014	48–91	273–292	627	91	34.6	26[b]	3.0

[a] SOA yield ($Y_{\text{SOA}} = \Delta\text{OM}/\Delta\text{Iso}$) is calculated at the point of maximum organic mass (OM).
[b] In Exp. SO2, SO2(g) was injected into the chamber to generate acidic seeds instead of directly injecting H_2SO_4.

Figure 1. The overall schematic of the model applied to simulate isoprene SOA within UNIPAR. $C_{g,i}$, $C_{mix,i}$, and $C_{or,i}$ are the concentrations of of each lumping species, i, within the gas, single homogenously mixed (SHMP) aerosol, and organic-only aerosol, repestively. $K_{mix,i}$ and $K_{or,i}$ are the equilibrium partitioning coefficients for the SHMP and organic-only aerosol, respectively.

Figure 2. The stoichiometric mass coefficients of each lumping group at a VOC/NO$_x$ (ppbC ppb^{-1}) of 25.

Figure 3. Time profiles of the experimentally measured and simulated SOA mass concentrations resulting from the photooxidation of isoprene. Data from experiments peformed in the absence of inoroganic seed is shown in blue, in the presence of sulfuric acid in orange, and in the presence of inorganic seed generated from SO_2 photooxidation in green. Solid, dashed, and dashed-dotted lines represent the simulated total organic mass (OM_T), organic mass from aerosol phase reactions (OM_{AR}), and organic mass from partitioning (OM_P), respectively. The experimental measured organic mass (OM_{exp}) is shown with square markers and is corrected for particle wall loss. The VOC/NO_x (ppbC ppb^{-1}) are shown for each experiment.

Title Page

Abstract | Introduction

Conclusions | References

Tables | Figures

|◄ | ►|

◄ | ►

Back | Close

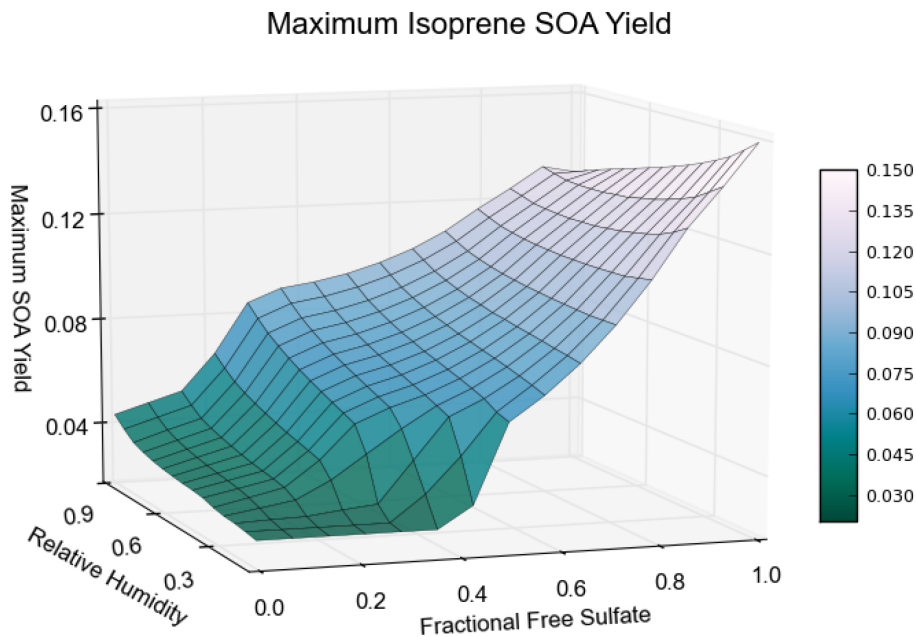Full Screen / Esc

Printer-friendly Version

Interactive Discussion
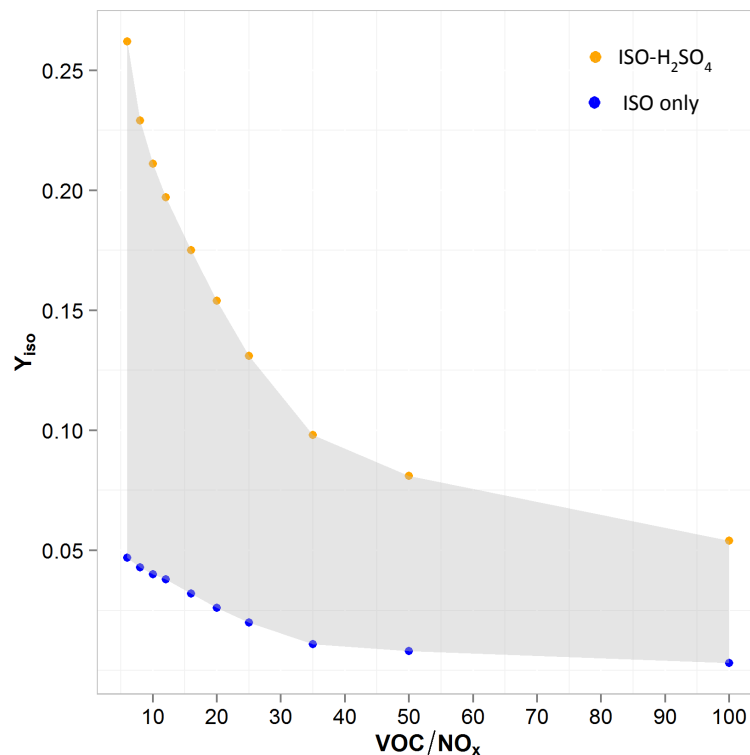
Figure 4. Simulated isoprene SOA yields (Y_{SOA} = ΔOM/ΔIso) as a function of VOC/NO$_x$ (ppbC ppb^{-1}) for values 10 to 100. The simulations were performed using the experimental conditions of SA1 (Table 1) without inorganic seed (blue) and in the presence of untitrated sulfuric acid (orange).

Figure 5. Simulated isoprene SOA yields (Y_{SOA} = ΔOM/ΔIso) as a function of relative humidity (RH) and fractional free sulfate (FFS = ([SO_4^{2-}] – 0.5[NH_4^+])/[SO_4^{2-}]). Using the experimental conditions of SA1, the RH and FFS were varied to determine the impact of acidity and aerosol liquid water content on Y_{SOA}.
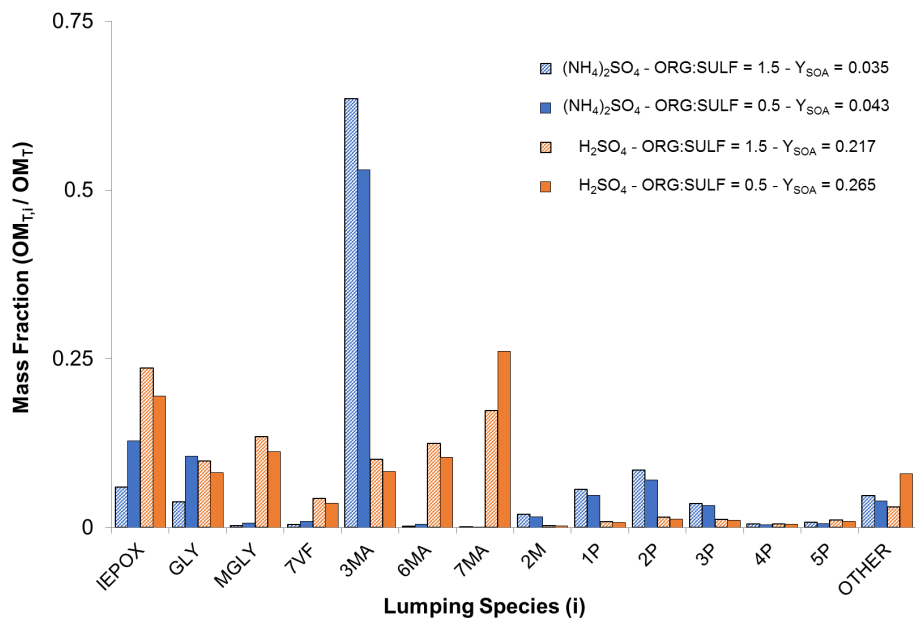
Figure 6. The mass fraction ($MF_i = OM_{T,i}/OM_T$) of lumping species, i, that contribute significantly to the simulated isoprene SOA in the presence of ammonium sulfate, $(NH_4)_2SO_4$, and sulfuric acid seeds, H_2SO_4, at organic to sulfur mass ratios of 0.5 and 1.5. The MF_i of the remaining lumping groups are summed and included in "OTHER." The MF_i, Y_{SOA}, and org:sulf are calculated at the point of maximum SOA mass. The meteorological conditions and isoprene consumption are based on the experimental conditions of SA1 performed on 27 January 2015 except for RH, which is set at 60 %.